Saturation Effects in Polarized Fluorescence Photobleaching Recovery and Steady State Fluorescence Polarization

Edward H. Hellen and Thomas P. Burghardt
Department of Biochemistry and Molecular Biology, Mayo Foundation, Rochester, Minnesota 55905 USA

ABSTRACT The time-resolved anisotropy produced in polarized fluorescence photobleaching recovery experiments has been successfully used to measure rotational correlation times in a variety of biological systems, however the magnitudes of the reported initial anisotropies have been much lower than the theoretically predicted maximum values. This small time-zero anisotropy has been attributed to fluorophore motion, wobble and rotation, during the photobleaching pulse. We demonstrate that inclusion of the possibility of saturation of the fluorophore's transition from its ground state to its excited state during the photobleaching pulse leads to the prediction of reduced time-zero anisotropy. This eliminates the need to rely solely on the assumption of fluorophore motion during the photobleaching pulse as the cause of the reduced initial anisotropy. We present theoretical and experimental results which show that the initial anisotropy decreases as both the bleach pulse intensity is increased and bleach pulse duration is decreased so as to keep the total integrated bleach pulse constant. We also show theoretical and experimental results demonstrating that at high excitation intensity the effects of saturation cause the steady state fluorescence polarization to decrease. We estimate that saturation may occur using common photobleaching conditions.

INTRODUCTION

The time-resolved anisotropy produced in polarized fluorescence photobleaching recovery (PFPR) experiments has been successfully used to measure rotational correlation times in a variety of biological systems: lipid probe rotation in membranes (Smith et al., 1981); internal motions of DNA (Scalettar et al., 1988, 1990); acetylcholine receptor rotation in cell membrane (Velez and Axelrod, 1988; Velez et al., 1990); rotation of antibodies and lipids associated with phospholipid monolayers (Timbs and Thompson, 1990); and internal dynamics of chromatin in intact nuclei (Selvin et al., 1990). However the magnitudes of the reported initial anisotropies have been much lower than the theoretically predicted maximum values. This small time-zero anisotropy has been attributed to fluorophore motion, wobble and rotation, during the photobleaching pulse. We demonstrate that inclusion of saturation effects during the photobleaching pulse leads to the prediction of reduced time-zero anisotropy, thereby eliminating the need to rely solely on the assumption of fluorophore motion during the photobleaching pulse as the cause of reduced initial PFPR anisotropy.

We present theoretical and experimental results which show that the time-zero PFPR anisotropy decreases as both the intensity of the photobleaching pulse is increased and duration of the pulse decreased so as to keep the total integrated bleach pulse constant. The theoretically predicted intensity dependence is due to our inclusion of the possibility of saturation of the fluorophore's transition from its ground state to its first excited electronic state during the photobleaching pulse. Previous standard photobleaching analysis does not include saturation and predicts no dependence of anisotropy on bleach intensity for bleaches of constant total integrated intensity.

If saturation effects are responsible for the decreased anisotropy then they should also be detectable in steady state fluorescence polarization (SSFP) measurements if the excitation intensity is high enough. We present theoretical and experimental results showing that at high intensity the SSFP does decrease.

The initial PFPR anisotropy depends on the extent of fluorophore tumbling during the bleach pulse. Therefore in order to investigate the anisotropy's dependence on intensity, and because bleach pulses of different durations were required, it was important to choose a system in which the fluorophore does not tumble. We used rhodamine B, rhodamine 110, and fluorescein in silicone vacuum grease which provides an isotropic distribution of nontumbling fluorophore.

We estimate that saturation effects may occur under common conditions used in PFPR experiments. In addition, saturation becomes more important at faster time scale PFPR experiments because those experiments need increasingly intense bleaches in order to compensate for the shorter duration of their bleach pulses.

THEORY

Here we calculate the effect on the PFPR anisotropy of allowing for saturation of the transition from the fluorophore's ground state to its excited state during the photobleaching pulse. We will show that saturation causes a decrease in the PFPR anisotropy. First we give a brief description of a PFPR experiment and the resulting anisotropy. Detailed theory of PFPR has been described previously (Smith et al., 1981; Velez and Axelrod, 1988; Timbs and Thompson, 1990; Wegener and Rigler, 1984; Dale, 1987).

Received for publication 9 September 1993 and in final form 21 December 1993

Address reprint requests to Edward H. Hellen at the Department of Biochemistry and Molecular Biology, Mayo Foundation, Rochester, MN 55905. Tel.: 507-284-2427; Fax: 507-284-9349; E-mail: hellen@mayo.edu.

0006-3495/94/03/891/07 $2.00

PFPR is used to measure the rotational correlation time of molecules or small particles labeled with a fluorescent probe. This is accomplished by using a brief intense flash of polarized light to preferentially photobleach fluorescent probes whose absorption dipoles are parallel to the bleaching beam's polarization. Relaxation of the resulting anisotropic distribution of bleached fluorophore is measured by monitoring the postbleach fluorescence with a constant low intensity polarized illumination. Two types of experiments are used, with the photobleach polarization parallel and perpendicular to the illumination polarization, yielding postbleach fluorescences $F_{\parallel}(t)$ and $F_{\perp}(t)$. These quantities are combined with the prebleach fluorescence F_{-} to form the PFPR anisotropy

$$r(t) = (\Delta F_{\parallel}(t) - \Delta F_{\perp}(t))/(\Delta F_{\parallel}(t) + 2\Delta F_{\perp}(t)) \quad (1)$$

where $\Delta F_{\parallel,\perp}(t) = F_{-} - F_{\parallel,\perp}(t)$. The PFPR anisotropy decays to zero as the orientational distribution of bleached fluorophore becomes uniform. This behavior is analogous to the decay of a standard emission anisotropy (fluorescence or phosphorescence) due to rotation. Note however that the PFPR anisotropy defined in Eq. 1 is constructed from a "pump-and-probe" technique and is therefore different from the usual emission anisotropy which is constructed from a "pump-only" technique. A detailed comparison of the PFPR anisotropy with other polarization techniques is given by Velez and Axelrod (1988). A notable difference is that the maximal possible value for the PFPR anisotropy for an isotropic immobile sample is 4/7, compared to 2/5 for a standard emission anisotropy.

For free tumbling in three dimensions Velez and Axelrod (1988) show that the PFPR anisotropy decay can be approximated by

$$r(t) = A \exp(-6D_r t), \quad (2)$$

where D_r is the rotational diffusion coefficient and A is related to the depth of the photobleach, the amount of wobbling of the fluorophore during the bleach, and the angle between the fluorophore's absorption and emission dipoles. The initial anisotropy $r(0)$ is determined by the two fluorescences immediately after the photobleach, $F_{\parallel}(t = 0) \equiv F_{0\parallel}$ and $F_{\perp}(t = 0) \equiv F_{0\perp}$.

We are interested in the effect of photobleach intensity on the initial anisotropy $r(0)$. In particular if the intensity and duration of the photobleaching pulse are varied so as to keep the total number of photons in the bleach pulse constant, how is $r(0)$ affected?

We assume a three-state model for the fluorophore consisting of a ground state S_0, an excited state S_1, and a photobleached state S_b as shown in Fig. 1. The photobleaching light is polarized thus causing the excitation from ground to excited state to depend on the angle γ between the absorption dipole and the bleach beam polarization. The three transitions are: excitations from ground to excited state with rate constant $k_e \cos^2 \gamma$; de-excitations from excited to ground state with rate k_f (including both radiative and nonradiative transitions); and a bleaching transition from the excited to the bleached state with rate k_b. The fast relaxation from higher vibrational states to the lowest vibrational state of S_1 is considered instantaneous. k_e is proportional to the excitation intensity and as such will be used as the variable to designate intensity. The absorption and emission dipoles are assumed to be parallel.

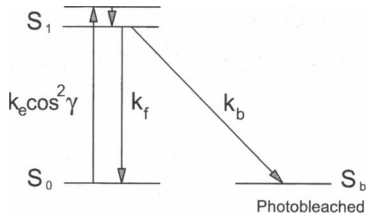

FIGURE 1 Three-state model used to describe the fluorophore. k_e is proportional to the laser excitation intensity. γ is the angle between the excitation polarization and the fluorophore's absorption dipole. k_f is the de-excitation rate back to the ground state S_0 due to both radiative and nonradiative transitions. k_b is the rate of transitions from S_1 to the photobleached state S_b. The vibrational relaxation shown within S_1 is assumed to be instantaneous compared to the other transitions.

Using the fact that for any fluorophore $k_f \gg k_b$ leads to the result for this three-state model that the concentration of unbleached fluorescent molecules at a particular orientation as a function of bleach intensity k_e and bleach duration τ is to a good approximation (see Appendix)

$$C(k_e, \tau, \gamma) = \exp\{-k_b \tau/[1 + k_f/(k_e \cos^2 \gamma)]\}. \quad (3)$$

Note that for photobleaching with a low intensity excitation ($k_e \ll k_f$) this becomes the familiar result for first order photobleaching,

$$C(k_e, \tau, \gamma) = \exp(-k_{eff}\tau), \quad (4)$$

where

$$k_{eff} = k_b k_e \cos^2 \gamma / k_f. \quad (5)$$

Now we can calculate the initial fluorescence intensities after the photobleach $F_{0\parallel}$ and $F_{0\perp}$ as a function of k_e and τ. The emission polarizer is set parallel to the low level illumination polarization at polar angle $\theta = 0$. For a bleach polarization parallel to the illumination polarization $\cos \gamma = \cos \theta$ so the initial postbleach fluorescence is

$$F_{0\parallel}(k_e, \tau) = 2\pi \int_0^{\pi/2} \sin \theta \cos^4 \theta \exp\left[-\frac{k_b \tau}{1 + k_f/(k_e \cos^2 \theta)}\right] d\theta. \quad (6)$$

For a bleach polarization perpendicular to the illumination polarization $\cos \gamma = \sin \theta \sin \phi$ so the initial postbleach fluorescence is

$$F_{0\perp}(k_e, \tau) = \int_0^{\pi/2} \sin \theta \cos^4 \theta \, N(\theta, k_e, \tau) \, d\theta. \quad (7)$$

where

$$N(\theta, k_e, \tau) = \int_0^{2\pi} \exp\left[-\frac{k_b \tau}{1 + k_f/(k_e \sin^2 \theta \sin^2 \phi)}\right] d\phi. \quad (8)$$

$F_{0\parallel}(k_e, \tau)$ and $F_{0\perp}(k_e, \tau)$ were calculated as a function of photobleaching intensity for bleaches of constant total integrated intensity by varying k_e and τ so as to hold the quantity $k_e\tau$ constant at 10^4. The rates of bleaching and de-excitation were set by $k_f/k_b = 10^4$. Using these values in Eq. 4 gives a bleach depth parameter of 1 in the low intensity bleaching term,

$$\exp(-1.0\cos^2\gamma), \tag{9}$$

which represents a common experimental bleach depth. Fig. 2 shows the theoretical PFPR anisotropy $r(0)$ that results from using Eq. 3, as a function of the normalized bleaching intensity k_e/k_f. Also shown is the constant time-zero PFPR anisotropy which results if saturation is ignored and Eq. 9 is used for the unbleached concentration. Note that when saturation is included $r(0)$ drops dramatically as k_e increases past k_f.

Here we show that in a common PFPR experiment it is possible to be in the situation where $k_e \sim k_f$ thus causing reduced initial anisotropy. The rate of absorptions per second k_e is

$$k_e = I \times \sigma, \tag{10}$$

where I is the number of photons per second per unit area for the bleaching beam, and σ is the absorption cross-section for the fluorophore. For a 200-mW, 514-nm photobleaching beam focused to 1 μm^2 and $\sigma = 1$ Å^2, one calculates that $I = 5 \times 10^{17}$ photons/(s $\times$ μm^2) and $k_e = 5 \times 10^9$ s^{-1}. A typical fluorescence lifetime is a few nanoseconds which gives $k_f \sim 3 \times 10^8$ s^{-1}. So even with only a 200-mW bleaching beam it is possible to have $k_e \sim 10 \times k_f$, thus demonstrating the potential importance of the considerations in this paper to the interpretation of PFPR results.

Here we calculate the effect on the SSFP of allowing saturation of the transition from the fluorophore's ground state to its excited state. We will show that saturation causes a decrease in the SSFP. Let $K = k_e/k_f$ be a normalized excitation intensity, where k_e and k_f are the excitation and de-excitation rates as defined above. Then the fraction of the fluorophores in the excited state as a function of the excitation intensity and the angle γ between the excitation polarization and the absorption dipole is

$$K\cos^2\gamma/(1 + K\cos^2\gamma). \tag{11}$$

The fluorescence polarization P is defined as

$$P(K) = [I_\parallel(K) - I_\perp(K)]/[I_\parallel(K) + I_\perp(K)], \tag{12}$$

where $I_\parallel(K)$ and $I_\perp(K)$ are measured fluorescence intensities where the emission polarizer is parallel and perpendicular, respectively, to the excitation polarization. In our experimental setup the excitation and emission paths are parallel. For an isotropic sample such as fluorescein or rhodamine in vacuum grease and making the approximation that the absorption and emission dipoles are parallel, the fluorescence intensities are

$$I_\parallel(K) = 2\int_0^{\pi/2} \sin\gamma\cos^2\gamma\left(\frac{K\cos^2\gamma}{1 + K\cos^2\gamma}\right)d\gamma \tag{13}$$

$$I_\perp(K) = \int_0^{\pi/2} \sin^3\gamma\left(\frac{K\cos^2\gamma}{1 + K\cos^2\gamma}\right)d\gamma. \tag{14}$$

$I_\parallel(K)$ and $I_\perp(K)$ were calculated as a function of the normalized excitation intensity K. Fig. 3 shows the resulting theoretical polarization as a function of K. At low intensity excitation K is small and the polarization is the typically measured value. When the excitation rate k_e equals $0.1 \times k_f$ the polarization is still within a few percent of its maximal value. As K increases, the ground state becomes depleted for those molecules whose absorption dipoles are parallel to the excitation polarization. This orientation dependent ground

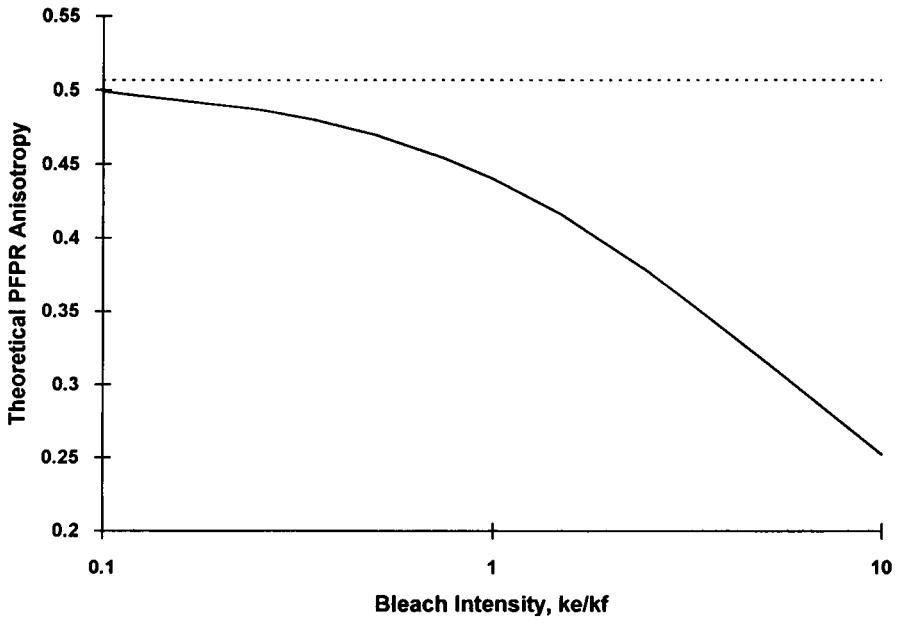

FIGURE 2 Theoretical time-zero PFPR anisotropy calculated including saturation (*solid line*) and neglecting saturation (*dashed line*) versus photobleaching excitation intensity, k_e/k_f, for bleaches of constant total integrated bleach intensity. Parameters used in the calculation are given in the text.

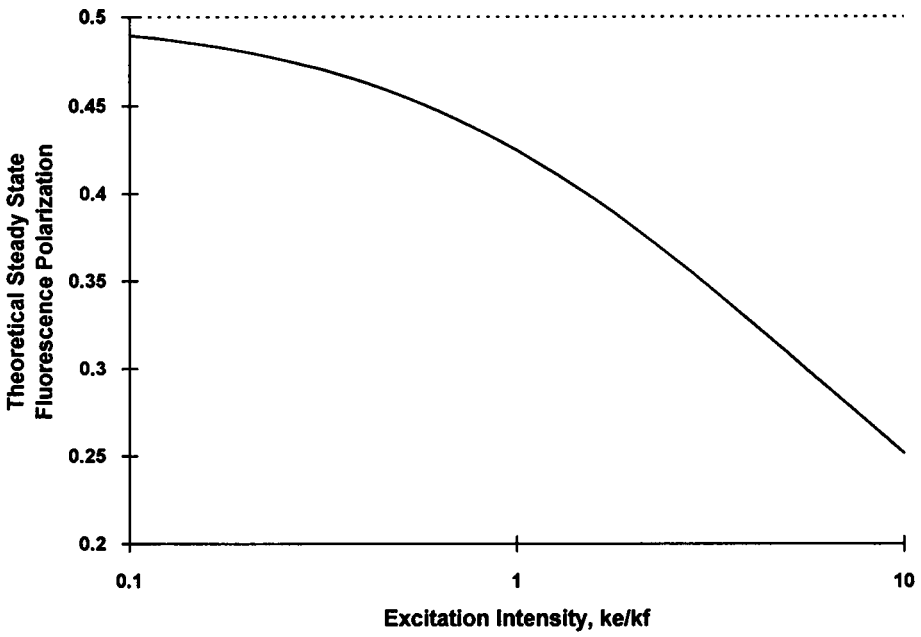

FIGURE 3 Theoretical steady-state fluorescence polarization calculated including saturation (*solid line*) and neglecting saturation (*dashed line*) versus excitation intensity, $K = k_e/k_f$.

state depletion causes a decrease in the polarization. When k_e is $10 \times k_f$ the polarization has decreased by 50%. Also shown in Fig. 3 is the constant polarization predicted if saturation is ignored corresponding to using

$$K \cos^2 \gamma, \tag{15}$$

in place of Eq. 11 for the population in the excited state used in Eqs. 13 and 14.

In this model for SSFP we have not included photobleaching. This is justified if the polarization measurements are made by rapidly switching the excitation polarization between parallel and perpendicular to the emission polarizer. In this way photobleaching will be uniform causing a decrease in the unbleached fluorophore concentration but not affecting the polarization ratio.

MATERIALS AND METHODS

Sample preparation

Rhodamine B, rhodamine 110, and fluorescein were each dissolved in ethanol at about 1 mg/ml. Drops of the dissolved fluorophore were mixed into silicone vacuum grease (Dow Corning High Vacuum Grease) until the grease was slightly colored, nominally 20 μM. In some cases the grease was then heated to help remove air bubbles. A layer of the grease < 1 mm was placed between quartz slides.

Optics

An argon ion laser (Coherent Innova 90; Palo Alto, CA) at either 488 or 514 nm depending on the fluorophore was used for fluorescence excitation and photobleaching. Two acousto-optic modulators (IntraAction ME-40; Bellwood, IL) in series were used to control laser beam intensity. After the modulators the beam passed through a spatial filter (25 μm)/beam diameter reducer, then through a Pockels Cell (Lasermetrics EOM-3079; Englewood, NJ) to control polarization. Epi-illumination on an upright microscope (Zeiss Axioplan, Oberkochen, Germany), equipped with a 20×, 0.5 NA, Zeiss Plan-Neofluar air objective, was used to focus the laser beam onto the sample. Fluorescence collected by the objective passed through the dichroic mirror, a barrier filter, an emission polarizer, and an image plane diaphragm to another objective which focused the fluorescence onto the active area of a photodiode detector module (EG&G Optoelectronics SPCM-200-PQ; Vaudreuil, Quebec, Canada). Sample position was controlled using an automated xy-translating stage (Ludl Electronics Products Ltd., Hawthorne, NY).

Intensities of the parallel and perpendicular polarizations were checked by passing the laser beam through the sample plane and through neutral density filters onto a photodiode. Intensities were equalized by independently setting their voltages sent to the acousto-optic modulator driver.

Laser beam power was 600 mW exiting the laser. The maximum power at the sample plane on the microscope was 200 mW. In PFPR experiments the bleach intensity was decreased, while bleach duration was increased in order to keep the total integrated bleach constant. Bleach durations used ranged from 100 μs to 40 ms.

For SSFP experiments neutral density filters were placed in front of the detector in order to give a count rate of 20,000 to 100,000 cps. Neutral density filters were also used to provide excitation intensities of 1.0 (full intensity), 0.1, 0.01, and 0.001.

Data collection

Photon counts from the photodiode detector module were counted by a counter/timer board (Keithley MetraByte CTM-05; Taunton, MA) in a 486 PC. A custom written Fortran and assembly language program (a modified version of a program generously provided by Dan Axelrod, University of Michigan, Ann Arbor) controlled the PFPR experiment and collected the data. A separate custom program ran the SSFP experiments.

In the SSFP experiments a square wave was used to alternately switch the excitation polarization between parallel and perpendicular so that any photobleaching would be independent of orientation. The xy stage translator was used to collect fluorescence at many positions, for less than 1 ms at each position. The highest frequency used for the square wave was 200 kHz. At this frequency the output from our custom built high voltage amplifier which drives the Pockels Cell was significantly rounded. This caused the measured polarizations to be less than what would be obtained with ideal square wave switching of the polarizations. As a check, low excitation intensity polarization measurements made with 250-Hz polarization switching gave values in the range of 0.40 to 0.45.

RESULTS

Fig. 4 shows PFPR anisotropies as a function of the photobleaching intensity. The bleach intensity k_e and bleach du-

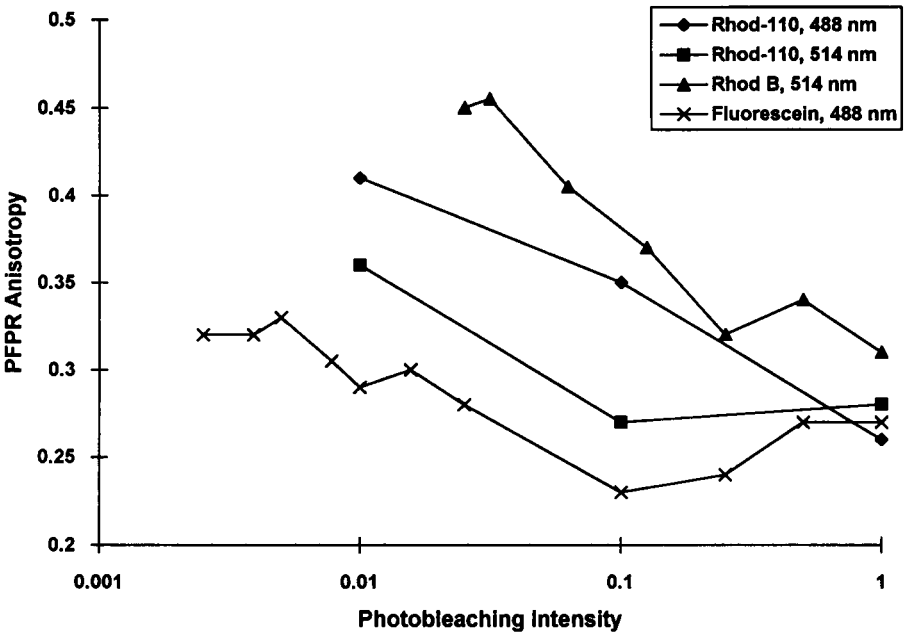

FIGURE 4 Measured PFPR anisotropies for various fluorophore in silicone vacuum grease as a function of photobleaching excitation intensity for bleaches of constant total integrated intensity. All anisotropy uncertainties are ±0.02. For each curve the highest bleach intensity was set equal to 1.

ration τ were varied so as to keep the total integrated bleach intensity $k_e\tau$ constant. Results are shown for rhodamine 110 in vacuum grease with the laser at 488 and 514 nm, for rhodamine B at 514 nm, and for fluorescein at 488 nm.

Fig. 5 shows SSFP measurements as a function of excitation intensity. Results are shown for rhodamine 110 in vacuum grease with the laser at 488 and 514 nm, for rhodamine B at 514 nm, and for fluorescein at 488 nm. These results were obtained using a 50-μs period for alternating between parallel and perpendicular excitation polarization. When the polarization switching period was increased to 4 ms the low intensity polarization for rhodamine 110 increased to 0.40. For fluorescein and rhodamine B the low intensity polarization with a 4-ms polarization switching period was 0.45.

Fig. 6 shows the PFPR anisotropy as a function of time for rhodamine B in vacuum grease with a full intensity photobleach. This is from one set of runs and is representative of the PFPR anisotropy results for the different fluorophores and different photobleaching intensities.

A comparison of the silicone vacuum grease samples with and without fluorophore showed that samples with fluorophore were 800 times more fluorescent than pure vacuum grease samples. Therefore there was no spectroscopic contribution from the vacuum grease.

DISCUSSION

The PFPR results in Fig. 4 all show a decreasing anisotropy as bleaching intensity increases. This is in agreement with the

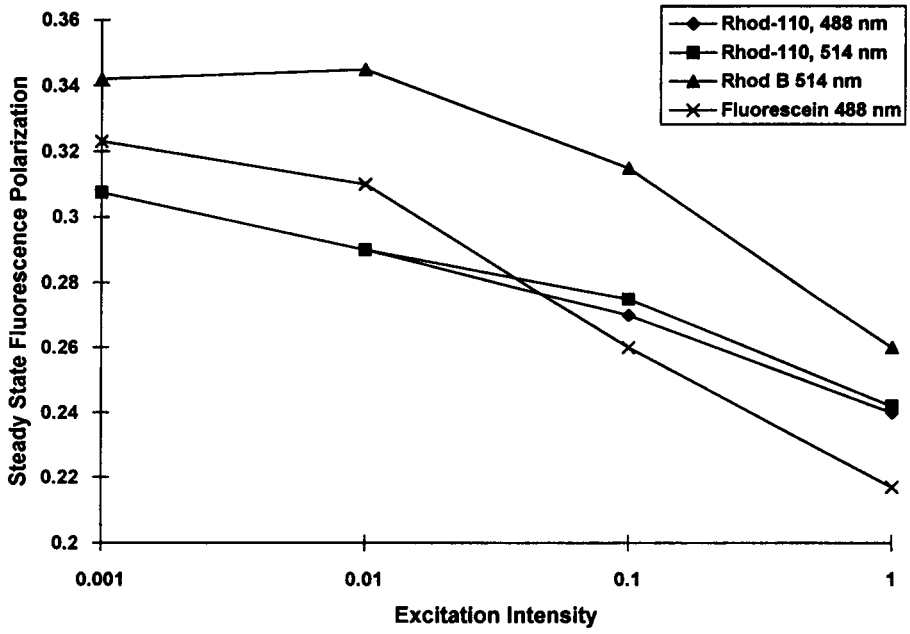

FIGURE 5 Measured steady state fluorescence polarization for various fluorophore in vacuum grease as a function of excitation intensity. All polarization uncertainties are ±0.01. For each curve the highest excitation intensity was set equal to 1.

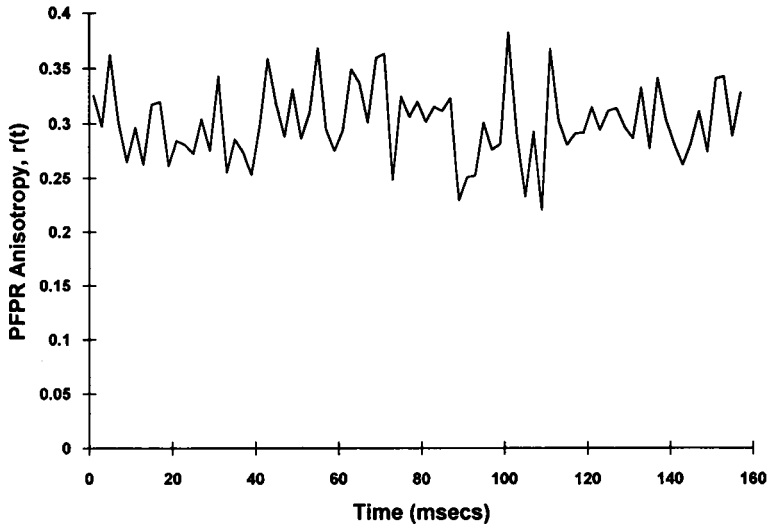

FIGURE 6 PFPR anisotropy raw data as a function of time for rhodamine B in silicone vacuum grease with a full intensity photobleach.

prediction of the three-state model shown in Fig. 2. Differences between the shapes of the experimental and theoretical curves may be due to additional transitions and photochemical processes which are not included in our simple three-state model. For example we do not include the possibility that a fluorophore in the excited state S_1 may absorb a photon, and we ignore the possibility of reversible photobleaching. But our model does include the important feature of saturation which predicts the observed intensity-dependent PFPR anisotropy.

Previously, low time-zero PFPR anisotropies have been explained solely by motion occurring during the bleach pulse, either wobbling of the fluorophore or rotation of the fluorophore labelled molecule. Typical reported time-zero anisotropies are 0.10 to 0.30 with corresponding wobble angles of 35 to 60° (Scalettar et al., 1988, 1990; Velez and Axelrod, 1988; Velez et al., 1990; Timbs and Thompson, 1990; Selvin et al., 1990). However Fig. 2 shows that the maximum PFPR anisotropy for the commonly used bleach depth parameter of 1 is about 0.50. In this paper we demonstrate that saturation effects during the bleach pulse are another potential reason why measured PFPR anisotropies are far below this maximum.

The PFPR anisotropies were found to be constant in time as shown in the representative example of Fig. 6. This confirms our assumption that fluorophore in silicone vacuum grease does not tumble and justifies the use of different bleach durations.

Here we compare fluorophore wobble angles calculated from experimental results taking saturation into account with those calculated ignoring saturation. The fluorophore wobbling is modeled by the absorption dipole being confined to a cone whose half angle is the wobble angle (Scalettar et al., 1988; Velez and Axelrod, 1988). For rhodamine 110 the high intensity PFPR anisotropy was 0.27. If saturation is ignored, this requires a wobble angle of about 40°. By considering saturation one finds that rhodamine 110's nonsaturated PFPR anisotropy is about 0.38 which requires a smaller wobble angle of about 30°. This value can be compared to the wobble angle deduced from standard low intensity SSFP measurements which report on motion occurring at the faster time scale of the fluorescence lifetime. In our experiments the low intensity SSFP values are 0.40 to 0.45 from which we deduce wobble angles of 15 to 25°. So by taking saturation into account the PFPR-deduced wobble angle and the SSFP wobble angle are in closer agreement than if saturation is ignored. Note that it is expected that the PFPR wobble angle should be greater than or equal to the SSFP wobble angle, since the former detects wobbling during the bleach, which is typically tens of microseconds to tens of milliseconds, whereas the latter detects wobbling during the much shorter fluorescence lifetime. Here we have assumed the absorption and emission dipoles are parallel. We could have attributed some or all of the 15 to 25° angle deduced from SSFP to a nonzero angle between absorption and emission dipoles, but this would not have changed any of our conclusions about how saturation affects the PFPR anisotropy.

We also investigated the effect of high excitation intensity on the SSFP. Fig. 3 shows that inclusion of saturation leads to the prediction that the polarization decreases as a function of excitation intensity. The measured polarizations in Fig. 5 for the various fluorophores in vacuum grease show the predicted intensity-dependent decrease. The measured magnitude of the polarizations in these experiments is also reduced due to the rapid switching of the excitation polarization as explained under Materials and Methods. However the measured decrease in polarization as a function of excitation intensity is real.

In this paper we have demonstrated that saturation during the photobleaching pulse causes decreases in the time-zero PFPR anisotropy. We have also shown that the situation of $k_e \sim k_f$ where saturation is important is attainable under ordinary photobleaching conditions. Therefore it seems likely that saturation effects, in addition to fluorophore wobbling and tumbling, may be responsible for PFPR anisotropies being lower than those predicted using

the usual first order bleaching term of Eq. 4 which does not include saturation. If saturation is taken into account then the fluorophore wobble angle deduced from time-zero PFPR anisotropy and that deduced from low intensity SSFP measurements are in closer agreement than if saturation is ignored.

APPENDIX

Here we calculate the concentration of remaining unbleached fluorophore as a function of the intensity k_e and duration of the photobleaching pulse τ for the three-state model of Fig. 1.

$$S_0 \underset{k_f}{\overset{k_e}{\rightleftharpoons}} S_1 \overset{k_b}{\rightarrow} S_b \tag{A1}$$

(In the derivation we drop the $\cos^2 \gamma$ from the excitation term.) The corresponding differential equations for the populations of the three states are,

$$\frac{dS_b}{d\tau} = k_b S_1 \tag{A2}$$

$$\frac{dS_1}{d\tau} = k_e S_0 - (k_f + k_b) S_1 \tag{A3}$$

$$\frac{dS_0}{d\tau} = k_f S_1 - k_e S_0 \tag{A4}$$

We are interested in the population of the unbleached fluorophore at the end of a bleaching pulse of duration τ,

$$C(\tau) = S_0(\tau) + S_1(\tau) \tag{A5}$$

S_0 and S_1 are easily solved for by taking Laplace transforms of the differential equations and using the initial condition $S_0(0) = 1$, $S_1(0) = S_b(0) = 0$. The results are

$$S_0(\tau) = \frac{(a - k_f - k_b)e^{-a\tau} + (k_f + k_b - b)e^{-b\tau}}{a - b} \tag{A6}$$

$$S_1(\tau) = \frac{k_e(e^{-b\tau} - e^{-a\tau})}{a - b} \tag{A7}$$

where

$$a = \frac{k_e + k_f + k_b}{2} + \sqrt{\left(\frac{k_e + k_f + k_b}{2}\right)^2 - k_e k_b} \tag{A8}$$

$$b = \frac{k_e + k_f + k_b}{2} - \sqrt{\left(\frac{k_e + k_f + k_b}{2}\right)^2 - k_e k_b} \tag{A9}$$

Typically $k_f > 10^4 k_b$, therefore the above equations can be approximated by

$$a = k_e + k_f \tag{A10}$$

$$b = \frac{k_b}{1 + k_f/k_e} \tag{A11}$$

Thus $a \gg b$, so that the initial transient terms in $S0$ and $S1$ can be neglected resulting in the good approximation

$$C(\tau) = \exp\left(\frac{-k_b \tau}{1 + k_f/k_e}\right) \tag{A12}$$

Reinserting the $\cos^2 \gamma$ into the excitation term gives Eq. 3.

We thank Predrag Ilich and W. David Braddock for helpful discussions and Elena Klimtchuk for critically reading the manuscript.

This work was supported by the National Institutes of Health (R01 AR 39288), the American Heart Association (Grant in Aid 93006610), and the Mayo Foundation. T. P. B. is an Established Investigator of the American Heart Association.

REFERENCES

Dale, R. E. 1987. Depolarized fluorescence photobleaching recovery. *Eur. Biophys. J.* 14:179–193.

Scalettar, B. A., P. R. Selvin, D. Axelrod, J. E. Hearst, and M. P. Klein. 1988. A fluorescence photobleaching study of the microsecond reorientational motions of DNA. *Biophys. J.* 53:215–226.

Scalettar, B. A., P. R. Selvin, D. Axelrod, M. P. Klein, and J. E. Hearst. 1990. A polarized photobleaching study of DNA reorientation in agarose gels. *Biochemistry.* 29:4790–4798.

Selvin, P. R., B. A. Scalettar, J. P. Langmore, D. Axelrod, M. P. Klein, and J. E. Hearst. 1990. A polarized photobleaching study of chromatin reorientation in intact nuclei. *J. Mol. Biol.* 214:911–922.

Smith, L. M., R. M. Weis, and H. M. McConnell. 1981. Measurement of rotational motion in membranes using fluorescence recovery after photobleaching. *Biophys. J.* 36:73–91.

Timbs, M. M., and N. L. Thompson. 1990. Slow rotational mobilities of antibodies and lipids associated with substrate-supported phospholipid monolayers as measured by polarized fluorescence photobleaching recovery. *Biophys. J.* 58:413–428.

Velez, M., and D. Axelrod. 1988. Polarized fluorescence photobleaching recovery for measuring rotational diffusion in solutions and membranes. *Biophys. J.* 53:575–591.

Velez, M., K. F. Barald, and D. Axelrod. 1990. Rotational diffusion of acetylcholine receptors on cultured rat myotubes. *J. Cell Biol.* 110: 2049–2059.

Wegener, W. A. 1984. Fluorescence recovery spectroscopy as a probe of slow rotational motions. *Biophys. J.* 46:795–803.

Wegener, W. A., and R. Rigler. 1984. Separation of translational and rotational contributions in solution studies using fluorescence photobleaching recovery. *Biophys. J.* 46:787–793.